ELSEVIER

Ultrasonics xxx (2002) xxx–xxx

Ultrasonics

www.elsevier.com/locate/ultras

Photorefractive interferometers for ultrasonic measurements on paper

Emmanuel F. Lafond [a,*], Pierre H. Brodeur [a], Joe P. Gerhardstein [a], Charles C. Habeger [a], Kenneth L. Telschow [b]

[a] Institute of Paper Science and Technology, 500 10th Street, N.W, Atlanta, GA 30318-5794, USA
[b] Idaho National Engineering and Environmental Laboratory, Lockheed Martin Idaho Technologies Co. Idaho Falls, ID 83415-2209, USA

1. Introduction

Photorefractive interferometers have been employed for the detection of ultrasound in metals and composites since 1991 [1–4]. Instances of laser-generated ultrasound and laser-based detection in paper were reported in 1996 [5]. More recently, bismuth silicon oxide (BSO) photorefractive interferometers were adapted to detect ultrasound in paper [6]. In this article we discuss BSO and GaAs photorefractive detection of ultrasound on different paper grades and present the resulting waveforms.

Compared to contact piezoelectric transducer methods, laser interferometry offers significant advantages. One of these is that it is a noncontact technique. This is especially important for on-line application to lightweight papers which could be marked or damaged by contact transducers. Broadband ultrasonic laser generation matched with the broadband sensitivity of laser interferometers is another benefit. This is important for obtaining narrow pulses in nondispersive time-of-flight determinations and for measuring the phase velocity of dispersive modes over a wide frequency band. Also, laser ultrasonic techniques provide a measure of bending stiffness through the analysis of low frequency A_0 waves.

2. Detection of ultrasonic waves in paper

From a mechanical point of view, paper is a very anisotropic medium. It is roughly twice as stiff along the direction of its manufacture (or machine) direction (MD) than along the cross machine direction (CD), and it is two orders of magnitude less stiff in the thickness direction than it is in the in-plane directions. At frequencies below 1 MHz, the thickness is generally much less than the out-of-plane bulk mode wavelengths, and low-order Lamb waves propagate naturally. Because of the fibrous structure of paper [7] (about 40 μm diameter fiber), high frequency ultrasonic waves (<1 MHz) are greatly attenuated by Rayleigh scattering. Thus, paper ultrasound analyses are essentially limited to the first order symmetric Lamb wave (S_0) and the first order antisymmetric Lamb wave (A_0).

An A_0 wave at low frequencies mainly generates displacements perpendicular to the surface of the web. On the other hand, S_0 waves produce almost exclusively in-plane motions. The A_0 waves are dispersive at low frequency, whereas the S_0 waves are nondispersive. The frequency-dependent phase velocities of the first order A_0 wave are much smaller than the velocity of the first order S_0 wave. As generated and detected by laser methods, the amplitudes of the S_0 waves are much smaller than the amplitudes of the A_0 waves [8,9].

Sometimes, glossy-faced, coated papers are tested, but generally we must deal with bare fiber surfaces. The irregular character of the uncoated paper surface produces a major difficulty in the laser detection of ultrasound. The reflected speckle pattern results from the scattering of a coherent signal beam off a rough surface. Because paper is such a strongly scattering medium, the reflected light is diffused as well as speckled. Therefore, multiple-speckle interferometers are excellent candidates for paper applications. They collect light from many speckles and provide better sensitivity to ultrasonic displacements.

3. Photorefractive adaptive interferometers

Photorefractive [10,11] interferometers are multiple-speckle interferometers with potential applicability to highly scattering materials. They use a photorefractive crystal to interfere the planar wavefront of a pump beam with the speckled wavefront of a signal beam (beam

* Corresponding author: Tel.: +1-404-894-5700; fax: +1-404-894-4778.
E-mail address: emmanuel.lafond@ipst.edu (E.F. Lafond).

0041-624X/02/$ - see front matter © 2002 Published by Elsevier Science B.V.
PII: S0041-624X(02)00252-4

back-scattered from the surface of the paper). Different photorefractive techniques exist for wave mixing [11], with various levels of efficiency and response times to the changing speckle pattern. Listed in order of adaptation speed, these are the self-pumped phase-conjugate mirror (PCM) method, the double phase-conjugate mirror (DPCM) technique, the four-wave mixing (FWM) method [4], the two-wave mixing (TWM) technique, and the photoinduced-electromotive force (photo-EMF) technique.

In the TWM design [1,10] the pump and signal beams interfere to create an index grating inside a photorefractive crystal. Ultrasonic signals modulate the phase of the signal beam altering the interference between the signal beam and the diffracted pump beam. This modulates the intensity of light at a photodetector placed after the crystal. The photorefractive crystal does not respond fast enough to modify the diffraction pattern in accordance with the ultrasonic signal. Theoretically, each speckle from the signal beam is matched with a speckle from the reference beam. Hence, instead of relying on the low power of a single speckle (as does the Mach–Zehnder interferometer), all of the speckles collected by the input aperture contribute to the interference signal.

We attempted two photorefractive interferometer methods. One was a TWM technique and the other was a photo-EMF method. Only the experiments with the TWM technique are reported in this article. As described below, we performed laser ultrasonic measurements on paper with two different TWM interferometers. In both cases, the generation of ultrasound was achieved in a noncontact way with a pulsed Nd:YAG laser doubled or not at 532 nm or 1064 nm. Point and line source generation shapes were formed.

3.1. Detection in the visible with a BSO photorefractive interferometer

We used a bismuth silicon oxide ($Bi_{12}SiO_{20}$ or BSO) crystal [2,11] as the active element for our first approach. We chose BSO because of its high photorefractive gain, transparency in the visible spectrum, availability of green laser, uniformity of crystal production, and reasonable cost. The wavelength of the detection laser was 514.8 nm.

Figs. 1 and 2 detail the design of the BSO photorefractive interferometer. The beam coming from the detection laser was split into two beams (incident and pump), having orthogonal polarizations using a first $\lambda/2$ plate and a polarizing beamsplitter. This allowed the ratio of the power of the incident beam over the power of the pump beam to be adjusted. The incident beam was horizontally polarized before passing through the second polarizing beamsplitter, and through the $\lambda/4$ plate. Then, it was focused onto the paper sample into the shape of a circular spot by the microscope objective. In order to detect A_0 and S_0 waves simultaneously with a single objective, the angle between the incident/reflected beam and the perpendicular to the surface of the paper was set to 40°. The back-scattered light from the paper was collected by the same objective. After going through the $\lambda/4$ plate a second time, the speckles having a vertical polarization were reflected at an angle of 90° by the polarizing beamsplitter to provide the signal beam.

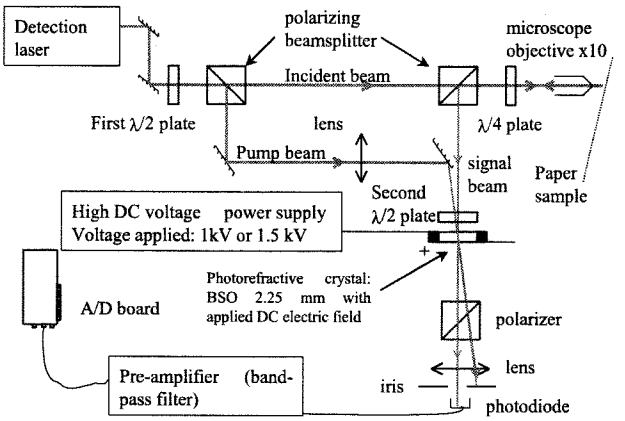

Fig. 1. Schematic of photorefractive interferometer using a BSO crystal with a DC applied voltage.

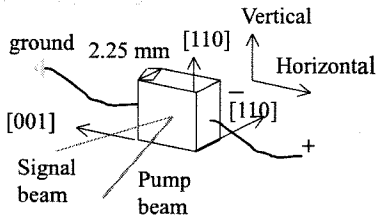

Fig. 2. Orientation of the axis of the BSO crystal in the photorefractive two-wave mixing interferometer.

The pump beam was reflected by a mirror and focused by a lens having a short focal length (38 mm) onto the edge of the second mirror. After the mirror, the beam was sufficiently expanded to illuminate the whole input surface of the photorefractive crystal. This was necessary because otherwise the high voltage applied to the sides of the crystal would concentrate the electric field into the areas not impinged by the pump beam.

The orientations of the crystallographic axis of the crystal are shown in Fig. 2. The signal and pump beams were in the horizontal plane and the photorefractive grating vector was along [0 0 1]. The dimensions of the crystal were 10 mm × 10 mm × 2.25 mm. The thickness was 2.25 mm, optimized for placing the polarization of the signal and reference beams at 90° to each other at the output of the crystal.

The pump and signal beams had their polarizations rotated by a second $\lambda/2$ plate before entering the crystal.

Because of the high coefficient of optical activity of BSO crystal (38°/mm at 515 nm), the polarization had to be rotated in order to optimize the sensitivity of the interferometer to the ultrasonic phase shift. The angle between the two beams was between 2° and 5°, which is appropriate for two-wave mixing when a high voltage is applied to the crystal.

The two beams (pump and signal) interfere in the crystal and create an index grating which diffracts the pump beam into a reference beam in the direction of the signal beam. Since the two beams did not have the same polarization at the output of the crystal, the polarizer after the crystal was oriented to decrease the power of the signal beam relative to the reference beam. A lens was used to focus the two beams (reference and signal) onto the sensitive surface of the photodiode. An iris prevented the nondiffracted light coming from the pump beam to add noise onto the photodiode. The iris also blocked the parasitic light pulse at 1064 nm coming from the generation laser.

The reference and signal beams interfered on the photodiode, and the voltage from the photodiode was sent to a preamplifier having a bandwidth of 13 kHz–6 MHz to remove its low frequency components. The signal was digitized at 10^7 samples per second using a 8-bit acquisition/digitization board. The A/D board was driven by a software developed at IPST using LabView 5.0.

The generation part of this first setup was classical in laser ultrasonic experiments. The energy of the Q-switched Nd:YAG laser at 1064 nm could be adjusted between 0 and 413 mJ per pulse thanks to the variable attenuator. The full width at half maximum (FWHM) of the laser pulse was 6 ± 1 ns.

3.2. Results with BSO interferometer

All results were obtained in a temperature and humidity controlled environment. Relevant parameters concerning the samples are presented in Table 1.

Fig. 3 represents a laser-generated waveform on 26-lb linerboard. The dispersive A_0 wave is clearly visible but the S_0 wave amplitude is too small to be detected. In the captions, HV stands for the high voltage applied across the width of the crystal (1 cm). The energy per pulse for the generation laser at 1064 nm is also provided.

Fig. 4 shows a waveform obtained on drawing paper which exhibits both A_0 and S_0 waves. Most of the measurements with this setup were made using an ablation mode for generation to obtain high amplitude signals. This was not satisfying for two reasons: first, the strong ablation mode damages the paper and generates waveforms of varying shapes; second, the strength of the acoustic source varies significantly with the number of shots consecutively made at the same spot. Therefore, efforts were made to increase the interferometer sensitivity and to reduce the damage to the paper by decreasing the power density of the generation beam.

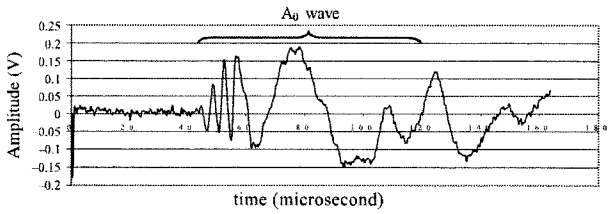

Fig. 3. 26-lb linerboard: displacement averaged four times with a generation–detection distance of 20 mm along MD, HV = 1.5 kV, 3.43 mJ/pulse.

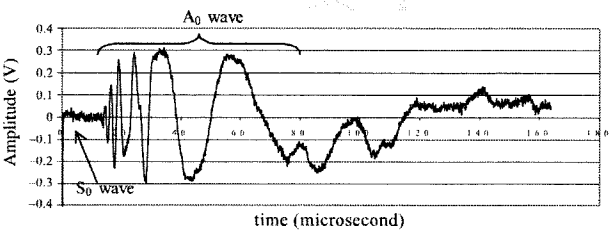

Fig. 4. Art (drawing) paper: displacement averaged three times with generation–detection distance of 10 mm along MD, HV = 1.5 kV, 0.65 mJ/pulse.

3.3. Detection in the infrared with a GaAs photorefractive interferometer

The schematic of the GaAs interferometer is presented in Fig. 5.

As in the case of the BSO crystal, we used the TWM method. However, no high voltage is applied to the crystal this time. This interferometer is easier to operate since GaAs is not optically active and there is need to adjust the incoming polarization.

The wavelength of the detection laser was 1064 nm. The incident power onto the paper was 138 mW and the power of the pump beam just before impinging the

Table 1
Thickness and grammage of paper grades investigated

Paper grade	Newsprint	Art paper	Copy paper	Sack	26-lb linerboard	42-lb linerboard	69-lb linerboard
Thickness (μm)	64	63	91	109	189	276	453
Grammage (g/m^2)	44	58	80	87	128	205	336

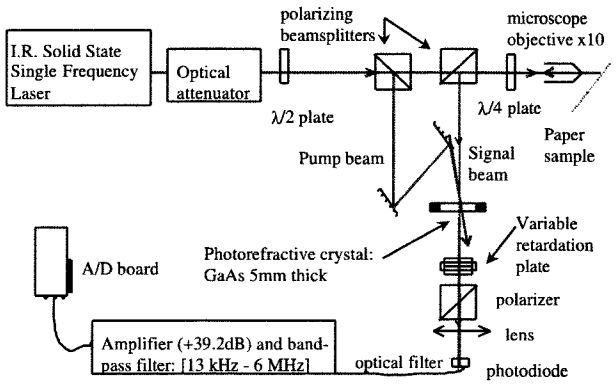

Fig. 5. Schematic of photorefractive interferometer using a GaAs crystal without applied voltage.

GaAs crystal was 95 mW. The power into the signal beam (scattered light collected by the microscope objective) was typically 1.7 mW.

The detection beam was incident at 45° to the normal to the paper surface. A line source was used for line generation. It was 25 mm long, 0.5 mm wide at its edges, and 1.0 mm wide at its center. Energy per pulse ranged from 49 to 72 mJ depending on the paper grade.

Measurements were obtained for laser generated waves traveling along the MD and the CD of the paper samples with generation–detection distances varying from 2 mm to 40 mm.

Figs. 6–14 present the waveforms obtained with the TWM GaAs interferometer: displacement (arbitrary units) as a function of time on various paper grades. The ratio of amplitudes of A_0 and S_0 waveforms varies from one paper to another but both waves are always present.

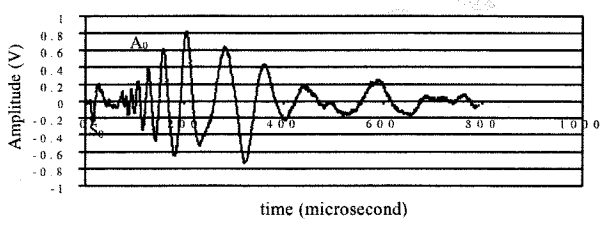

Fig. 6. Newsprint, 20 mm generation/detection distance, along CD, 56 mJ, single shot.

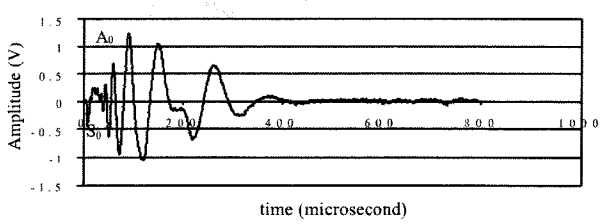

Fig. 7. Newsprint, 10 mm distance, along CD, 56 mJ, single shot.

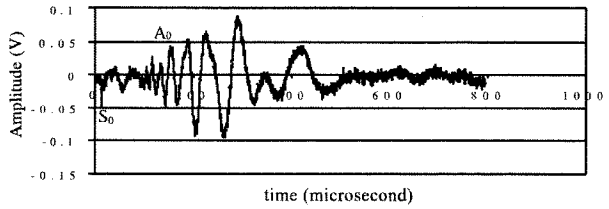

Fig. 8. Copy paper, 40 mm distance, along MD, 53 mJ, averaged ten times.

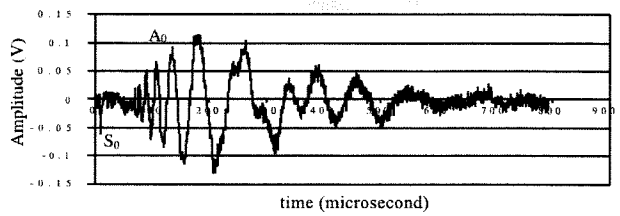

Fig. 9. Copy paper, 30 mm distance, along MD, 53 mJ, averaged four times.

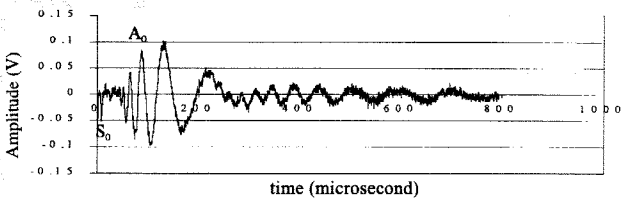

Fig. 10. Copy paper, 20 mm distance, along MD, 53 mJ, averaged ten times.

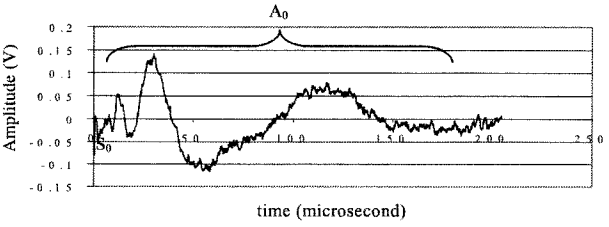

Fig. 11. Copy paper, 5 mm distance, along MD, 53 mJ, averaged four times.

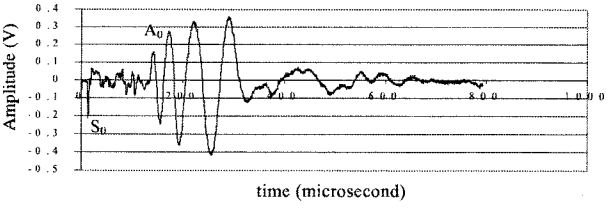

Fig. 12. Sack paper, 40 mm distance, along MD, 52 mJ, averaged four times.

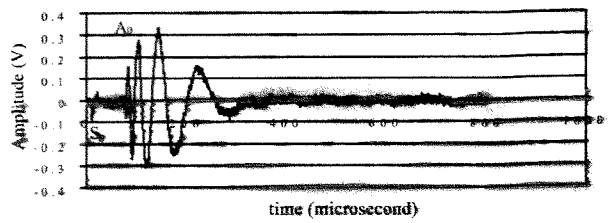

Fig. 13. 42-lb linerboard, 40 mm distance, along MD, 50 mJ, single shot.

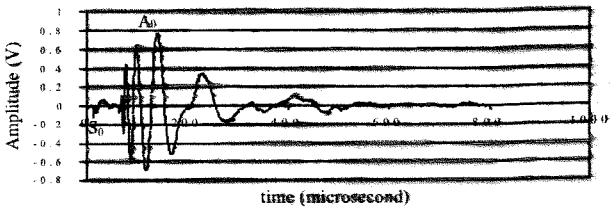

Fig. 14. 69-lb linerboard, 30 mm distance, along CD, 50 mJ, averaged four times.

4. Conclusions

Results of laser generation and interferometric detection of ultrasound on various static paper samples were presented. Seven very different paper grades were investigated. On all paper grades, the dispersive nature of the A_0 Lamb wave is clearly demonstrated.

A photorefractive interferometer using a GaAs crystal detected both A_0 and S_0 Lamb waves in single shot mode for the generation laser without leaving visible marks on the paper. Unlike single speckle interferometer implementations, the optimizations of the photorefractive interferometers were found to be insensitive to the orientation of the paper surface. The versatility of the interferometers was demonstrated by their optical and mechanical adaptability to very different paper grades.

The sensitivity of both interferometers could be improved using anti-reflection coated crystals, smaller f-number optics, and a photodiode with less noise. Since the semiconductor type crystals, such as GaAs, InP:Fe, or CdTe:V, have significantly shorter response times than BSO crystals, they should be preferred for TWM applications to a moving paper web. These crystals are able to adapt to the rapidly changing speckle pattern of a paper web impinged by a laser beam. The results presented in this paper argue that photorefractive interferometers hold promise for the mechanical characterization of paper in the laboratory and on-line on a paper machine.

Acknowledgements

The authors are pleased to thank the U.S. Department of Energy for its support with contract DE-FC07-97ID13578 on project "Laser Ultrasonic Web Stiffness Sensor".

The authors want to thank especially Dr. Kenneth L. Telschow and Mr. Vance A. Deason, both from the Idaho National Engineering and Environmental Laboratory (INEEL) for their help and advice in building the photorefractive interferometers.

References

[1] R. Ing, J.-P. Monchalin, Broadband optical detection of ultrasound by two-wave mixing in a photorefractive crystal, Appl. Phys. Lett. 59 (25) (1991) 3233–3235.
[2] T. Honda, T. Yamashita, H. Matsumoto, Optical measurement of ultrasonic nanometer motion of rough surface by two-wave mixing in $Bi_{12}SiO_{20}$, Japanese J. Appl. Phys. 34 Pt. 1 (7A) (1995) 3737–3740.
[3] B. Pouet, R. Ing, S. Krishnaswamy, D. Royer, Heterodyne interferometer with two-wave mixing in photorefractive crystals for ultrasound detection on rough surfaces, Appl. Phys. Lett. 69 (25) (1996).
[4] T. Hale, K. Telschow, V. Deason, Photorefractive optical lock-in vibration spectral measurement, Appl. Opt. 111 (1997) 8248–8258.
[5] M. Johnson, Investigation of the mechanical properties of copy paper using laser generated and detected lamb waves, Ph.D. Thesis, Georgia Institute of Technology (1996).
[6] E. Lafond, J. Gerhardstein, P. Brodeur, Non-contact characterization of static paper materials using a photorefractive interferometer, SPIE Conference on Nondestructive Evaluation Techniques for Aging Infrastructure and Manufacturing/Process Control and Sensors for Manufacturing, Newport, CA, SPIE 3589, 1999, pp. 31-41.
[7] C. Habeger, R. Mann, G. Baum, Ultrasonic plate wave in paper, Ultrasonics 17 (1979) 57–62.
[8] P. Brodeur, M. Johnson, Y. Berthelot, J. Gerhardstein, Noncontact laser generation and detection of lamb waves in paper, J. Pulp Paper Sci. 23 (5) (1997) J238–J243.
[9] M. Johnson, Y. Berthelot, P. Brodeur, L. Jacobs, Investigation of laser generation of Lamb waves in copy paper, Ultrasonics 34 (1996) 703–710.
[10] P. Yeh, Introduction to photorefractive nonlinear optics, John Wiley and Sons, NewYork, 1993.
[11] D. Nolte, Photorefractive effects and materials, Kluwer academic publishers, Boston, 1995.